

## Charged and magnetic fullerenes of silicon by metal encapsulation: Predictions from *ab initio* calculations

Vijay Kumar,<sup>1,2,3</sup> Abhishek Kumar Singh,<sup>2,\*</sup> and Yoshiyuki Kawazoe<sup>2</sup>

<sup>1</sup>Research Institute for Computational Sciences (RICS), National Institute of Advanced Industrial Science and Technology (AIST), Umezono 1-1-1, Tsukuba, 305-8568, Japan

<sup>2</sup>Institute for Materials Research, Tohoku University, Aoba-ku, Sendai 980-8577, Japan

<sup>3</sup>Dr. Vijay Kumar Foundation, 45 Bazaar Street, K. K. Nagar (West), Chennai 600 078, India

(Received 20 June 2006; published 13 September 2006)

Using *ab initio* calculations, we show that the encapsulation of Y, La, and Ac metal ( $M$ ) atom stabilizes the dodecahedral fullerene anion  $M@Si_{20}^-$  in the icosahedral symmetry. Similar to  $C_{60}$ , it is the ideal cage of silicon and the largest that can be stabilized by an  $M$  atom. Doping of other rare earths is further shown to stabilize magnetic dodecahedral fullerenes  $Pa@Si_{20}$ ,  $Sm@Si_{20}$ ,  $Pu@Si_{20}$ , and  $Tm@Si_{20}$  with  $1\mu_B$ ,  $4\mu_B$ ,  $4\mu_B$ , and  $3\mu_B$  spin magnetic moments, respectively, in contrast to most previous studies on  $M$ -encapsulated Si clusters in which the magnetic moment is completely quenched. The highest spin magnetic moment of  $7\mu_B$  is achieved for  $Gd@Si_{20}^-$  with half-filled  $4f$  states. The orbital magnetic moment is also calculated and it is  $\sim 1\mu_B$  in most cases. Neutral  $M@Si_{20}$  ( $M=Y, La, Ac, \text{ and } Gd$ ) behaves like superhalogen and interaction with a noble or alkali metal atom leads to salt like behavior. These findings could pave way for the realization of silicon fullerenes by doping of several elements.

DOI: [10.1103/PhysRevB.74.125411](https://doi.org/10.1103/PhysRevB.74.125411)

PACS number(s): 73.61.Wp, 36.40.Cg, 36.40.Wa, 73.22.-f

Nanostructures of silicon are currently of great interest because of future applications in nanodevices, sensors, silicon based optoelectronics, biological systems, and possibilities of new molecular structures. Much research has been done on elemental silicon clusters but no particular high stability cluster could be found.<sup>1</sup> Recently a major advance has been made by metal ( $M$ ) encapsulation which is a novel way to produce size selected cage clusters of silicon<sup>2-8</sup> and other elements<sup>6,7,9</sup> in high abundance. By choosing an appropriate  $M$  atom, properties of these clusters can be tuned. Cages with 10–16 atoms have been predicted<sup>2,4-7</sup> and high abundances have been obtained<sup>8,9</sup> for  $Ti@Si_{16}$  and  $Al@Pb_{12}^+$  almost exclusively, supporting the special stability of these clusters. Also a bulk phase of  $Pt@Pb_{10}$  has been synthesized.<sup>10</sup> The magnetic moments of the  $M$  atom in these clusters are generally completely quenched due to the strong interaction with the cage except for the icosahedral magnetic superatoms<sup>7</sup>  $Mn@Ge_{12}$  and  $Mn@Sn_{12}$ . Here we show that rare earth elements can be encapsulated in a  $Si_{20}$  cage to obtain silicon fullerenes with large magnetic moments. Further,  $M@Si_{20}$  ( $M=Y, La, Ac, \text{ and } Gd$ ) fullerene behaves like a superhalogen and the anion is predicted to be stabilized in high symmetry.

Several efforts<sup>11-16</sup> have been made in the past few years to stabilize a silicon fullerene but no evidence could be obtained as carbon fullerenes are predominantly  $sp^2$  bonded while silicon favors  $sp^3$  bonding. However, in  $C_{20}$ , the smallest fullerene of carbon with all pentagonal faces, the bonding is more  $sp^3$ -like, which makes the stabilization of  $C_{20}$  difficult but it suits well for  $Si_{20}$ . The presence of dangling bonds, however, makes the  $Si_{20}$  empty cage unstable. Encapsulation of an  $M$  atom could provide stability as in the case of smaller  $M@Si_n$  clusters.<sup>1-9</sup> Doping of a Zr atom was tried<sup>17</sup> in a dodecahedral  $Si_{20}$  cage and it leads to a large gain in the binding energy (BE) also. However, a Zr doped  $Si_{20}$  cage collapses<sup>2</sup> after optimization due to the relatively small size

of Zr atom and a  $Zr@Si_{16}$  fullerenelike cage was shown<sup>2</sup> to be the most appropriate. Doping of bigger atoms such as Pb, Sr, Ba, etc. leads to distorted  $M@Si_{20}$  cages<sup>18</sup> and relatively small endohedral doping energies that are unlikely to stabilize  $Si_{20}$  fullerene. Recently it has been shown<sup>19</sup> that an atom with an oxidation state of +4 is most suitable for the stabilization of  $Si_{20}$  fullerene and Th has been found to be the only element that fits well in the cage and leads to the high stability of the nonmagnetic neutral  $Th@Si_{20}$  fullerene with icosahedral symmetry. This is the ideal fullerene of Si as  $C_{60}$  is for carbon. Besides Th, many other rare earth elements have the appropriate atomic size to fit well in the  $Si_{20}$  cage, but their most favored oxidation state<sup>20</sup> is often +3 or +2 as the  $f$  orbitals are very well localized and the valence  $nd^1(n+1)s^2$  or  $nd^0(n+1)s^2$  electrons play the important role in bonding. Accordingly it could be possible to stabilize a silicon fullerene anion by these elements. We find that Y, La, and Ac atoms stabilize  $Si_{20}$  fullerene anion with  $I_h$  symmetry while magnetic silicon fullerenes can be produced in neutral as well as charged states by doping of some other rare earth elements.

The calculations have been performed using the *ab initio* projected augmented wave method<sup>21,22</sup> and a plane wave basis set within the spin-polarized density functional theory and the generalized gradient approximation<sup>23</sup> (GGA) for the exchange-correlation energy. For the  $M$  atoms we use pseudopotentials that treat all the valence orbitals including the  $f$  orbitals as well as the  $5s$  ( $6s$ ) and  $5p$  ( $6p$ ) core orbitals for the lanthanides (actinides). The clusters are placed in a large cubic unit cell and the Brillouin zone is represented by the  $\Gamma$  point. The conjugate gradient technique is used to optimize the structures without any symmetry constraints. The energy is considered to be converged when the force on each ion becomes  $0.001 \text{ eV/\AA}$  or less. The reliability of the pseudopotentials was tested<sup>19</sup> for bulk Si and other elements and good agreement was obtained with the experimental re-

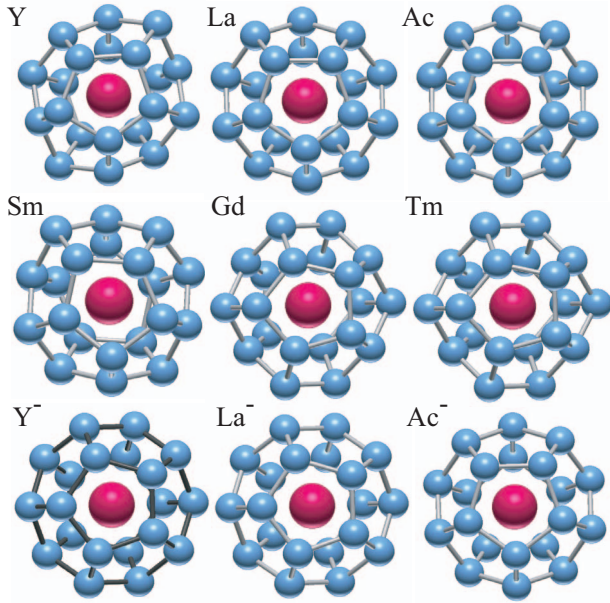


FIG. 1. (Color online) Optimized structures for neutral  $M@Si_{20}$ , ( $M=Y, La, Ac, Sm, Gd,$  and  $Tm$ ) and icosahedral  $M@Si_{20}^-$  anions ( $M=Y, La,$  and  $Ac$ ). Fullerenes with  $M=Ce, Pa^+, Pa, Np^+, Pu,$  and  $Gd^-$  have  $T_h$  symmetry as for  $Sm$  and  $Tm$  while the neutral fullerenes of  $Y, La, Ac,$  and  $Gd$  are Jahn-Teller distorted. Blue (magenta) balls show  $Si$  ( $M$ ) atoms.

sults. We considered two cages for  $Si_{20}$ : (i) the dodecahedral fullerene and (ii) a cage structure found in bulk  $Ce_5Mg_{42}$  phase.<sup>24</sup> The fullerene cage is found to be significantly lower in energy than the other isomer and here we present results for the fullerenes. Further calculations have been done with spin-orbit coupling and contribution from the orbital magnetic moments has also been obtained.

Figure 1 shows the optimized structures obtained for  $M=Y, La, Ac, Sm, Gd,$  and  $Tm$  in the neutral state. In all cases the icosahedral symmetry is reduced and the highest occupied-lowest unoccupied molecular orbital (HOMO-LUMO) gap is small ( $\sim 0.25$  eV). This can be seen in Fig. 2 (and also in Table I) in the case of  $M=Sm$  and  $Tm$ . The magnetic moments on these species are  $1\mu_B, 1\mu_B, 1\mu_B, 4\mu_B, 6\mu_B,$  and  $3\mu_B,$  respectively. For  $M=Ce, Pa, Sm, Pu,$  and  $Tm$ , the neutral fullerene cage has  $T_h$  symmetry with two slightly different Si-Si bond lengths of about  $2.320\pm 0.015$  Å and  $2.367\pm 0.008$  Å and two Si-M bond lengths of  $3.013\pm 0.037$  Å and  $3.385\pm 0.015$  Å. A dodecahedral structure can be viewed as a cube in which each face is capped by a pair of atoms. The pair of Si atoms has longer Si-Si and Si-M bond lengths (12 such Si atoms each with two short and one long Si-Si bonds). The Si-Si bond lengths are close to the value in bulk silicon. In other neutral cases, the cages are Jahn-Teller distorted but the charged clusters have a symmetric dodecahedral fullerene structure. For  $M=Y, La,$  and  $Ac$  the fullerene anion has the full  $I_h$  symmetry (Fig. 1) with the Si-Si (Si-M) bond lengths of 2.34 (3.27), 2.36 (3.31), and 2.38 (3.33) Å, and the HOMO-LUMO gap of 0.95, 0.82, and 0.85 eV, respectively (see Fig. 2 for  $La^-$ ). Therefore fullerenes are expected to be quite stable. The highest sym-

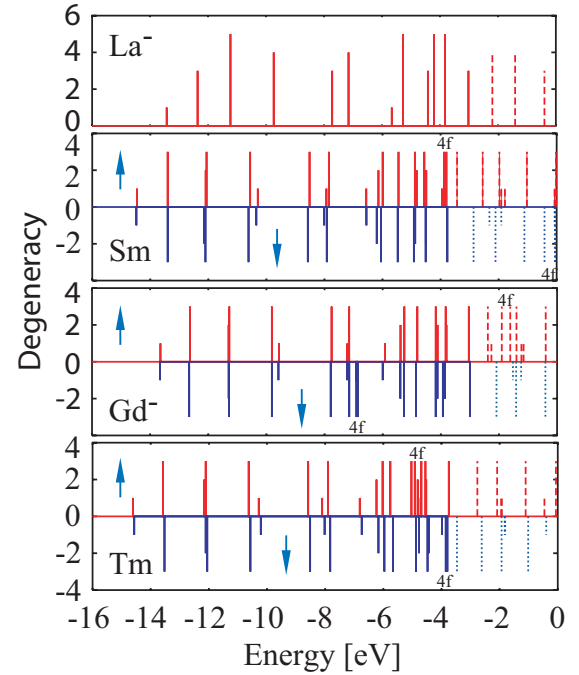


FIG. 2. (Color online) Electronic energy spectra of  $La@Si_{20}^-$ ,  $Sm@Si_{20}$ ,  $Gd@Si_{20}^-$ , and  $Tm@Si_{20}$  fullerenes. Broken lines show unoccupied states. Arrows correspond to the up- and the down-spin spectra. The general features of the spectra are similar except for the  $4f$  levels of the  $M$  atoms that are marked. These hybridize with the  $nF$  states of the Si cage. For  $La$  doped anion, the spectrum has icosahedral symmetry. However, in other cases the symmetry is reduced to  $T_h$  due to small changes in the bond lengths which lead to the splitting of the fivefold ( $H$ ) and fourfold ( $G$ ) symmetry states.

metry of these fullerenes makes them very special similar to  $C_{60}$ . In experiments clusters are often produced in charged state and we would expect high abundance of these fullerene anions. Further studies on  $Np@Si_{20}^-$  and  $Gd@Si_{20}^-$  show them to have  $T_h$  symmetry as in the case of  $M=Tm$  (Fig. 1). The Si-Si (Si-M) bond lengths in these fullerenes are 2.32 and 2.36 (2.99 and 3.39) Å and 2.34 and 2.38 (3.09 and 3.39) Å, respectively.  $Pm$  is isovalent to  $Np$  but the doped anion cage has nearly perfect  $I_h$  symmetry with Si-Si (Si-M) bond lengths of 2.33 (3.27) Å.

The BE with respect to free atoms, the HOMO-LUMO

TABLE I. The BE (eV/atom), HOMO-LUMO gap (eV), spin ( $\langle S_z \rangle$ ), and orbital ( $\langle L_z \rangle$ ) magnetic moments in  $\mu_B$ , and electron affinity (EA) in eV for  $M@Si_{20}$  fullerenes. For  $M=Gd$ ,  $\langle L_z \rangle$  is for anion.

$M$	BE	Gap	$\langle S_z \rangle$	$\langle L_z \rangle$	EA
Y	3.978	0.247	1	0	3.296
La	3.971	0.208	1	0	3.443
Pa	4.105	0.206	1	-0.37	3.539
Sm	3.880	0.334	4	-1.41	—
Gd	3.956	0.284	6	-0.20	3.321
Tm	3.857	0.282	3	2.41	—

gap, and the magnetic moments are given in Table I. The variations in the HOMO-LUMO gap for the anion fullerenes (Y, La, Ac, and Gd) and the BEs are small. Furthermore, the electron affinity in all these cases is nearly the same (3.30, 3.44, 3.54, and 3.32 eV, respectively) and it is close to the value for a Cl atom. Therefore, neutral fullerenes with encapsulation of these  $M$  atoms behave like *superhalogens*.

The electronic spectra of neutral  $M@Si_{20}$  ( $M=Sm$  and  $Tm$ ) and anion  $M@Si_{20}$  ( $M=La$  and  $Gd$ ) fullerenes are shown in Fig. 2. For  $M=La$ , the spectrum exhibits icosahedral symmetry. The electronic structures for  $M=Y$  and  $Ac$  are similar. The spectra have features as obtained for the case<sup>19</sup> of  $M=Th$ . The HOMO and the LUMO states have the  $T_{2u}$  and  $G_u$  symmetries, respectively. The electronic spectra as well as the bonding in these fullerenes can be understood<sup>19</sup> using a spherical model potential<sup>25</sup> due to the high symmetry of the cage. The dodecahedral  $Si_{20}$  cage has three  $\sigma$  bonds for each Si with neighboring Si atoms and these accommodate 50 electrons in  $1S$ ,  $1P$ ,  $1D$ ,  $1F$ , and  $1G$  orbitals (fully occupied). Ten electrons are in the  $1H$  orbitals that are partially occupied. Under the icosahedral symmetry the energy levels of  $1H$  orbitals split into a fivefold degenerate level which is fully occupied and two threefold degenerate levels that are empty. The remaining 20 valence electrons occupy  $sp^3$  hybrid orbitals that point outwards from the cage. In the spherical model the corresponding cage orbitals are  $2S$ ,  $2P$ , and  $2D$  that accommodate 18 electrons and are fully occupied while the  $2F$  orbitals are partially occupied with two electrons. In the  $I_h$  symmetry, the energy levels of  $2F$  orbitals split into a threefold degenerate HOMO ( $T_{2u}$ ) that accommodates two electrons and an empty fourfold degenerate  $G_u$  level. After  $M$  encapsulation, the four valence electrons (three from the trivalent  $M$  atom and one from charging of the cage) occupy the  $T_{2u}$   $2F$  hybridized orbitals completely leading to the stability of the fullerene anions.

For  $M=Sm$  ( $4f^66s^2$  configuration), the up-spin  $4f$  orbitals hybridize strongly with the up-spin  $2F$  orbitals of the cage and the seven fully occupied bonding states have very strong  $4f$  character ( $\sim 5.25$   $4f$  electrons). The antibonding up-spin states lie above the HOMO and are completely empty ( $4f$  contribution  $\sim 1.7e$ ). The remaining three electrons (two from the Si cage and one from Sm) are accommodated in the down-spin hybridized  $T_{2u}$  state which is fully occupied and forms the HOMO giving rise to net  $4\mu_B$  magnetic moments on this neutral fullerene. The valence of Sm is between 2 and 3. In the case of  $M=Pa$ , the  $2F$  cage orbitals hybridize with the  $4f$  orbitals of Pa. In the  $T_h$  symmetry the  $G_u$   $2F$  states split into a threefold degenerate state and a single state. The  $T_{2u}$  up- and down-spin states and the up-spin single state of  $G_u$  are occupied while the down-spin single state and the other threefold degenerate states are empty. The partial occupation of the  $2F$  states leads to small HOMO-LUMO gap. In the occupied hybridized state the  $4f$  contribution of Pa is about one electron and the remaining  $4f$  hybridized states lie above the HOMO giving rise to  $1\mu_B$  magnetic moment on this fullerene. Therefore Pa behaves like a tetravalent element. For  $M=Gd$  fullerene anion, all the down spin  $4f$  energy levels of Gd atom are occupied and the up-spin levels, empty. The remaining four electrons are used to fill the  $T_{2u}$   $2F$  cage orbitals as discussed above. This leads to  $7\mu_B$  mag-

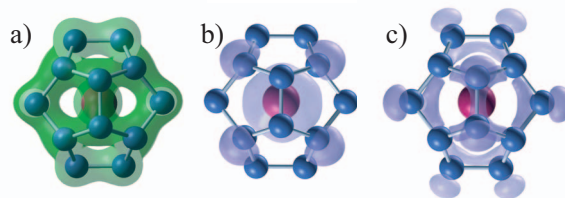


FIG. 3. (Color online) (a) Total pseudocharge density isosurface for  $Gd@Si_{20}^-$  shows covalent bonding as charge is concentrated in Si-Si bonds. (b) and (c) show the down- and up-spin magnetic polarizations. The magnetic moments are strongly localized around the Gd ion. Small polarization of the same spin is induced around the eight neighboring Si ions as in (b) while a small polarization of opposite spin is induced around the remaining twelve Si ions as in (c). Gd (Si) ion is shown in magenta (blue).

netic moment on this fullerene. This is the largest magnetic moment that can be obtained in these fullerenes by encapsulation of an atom. The exchange-splitting in the  $4f$  energy levels of Gd is the largest and as shown in Fig. 2 the  $4f$  occupied level lies significantly below the HOMO. Continuing the filling of the  $4f$  orbitals, in the  $4f^{13}6s^2$  configuration of Tm, all the up- and down-spin hybridized  $4f$  states ( $4f$  contribution  $\sim 12.5e$ ) and the up-spin  $T_{2u}$   $2F$  cage states are occupied while the hybridized down-spin  $T_{2u}$   $2F$  state are completely empty. This leads to  $3\mu_B$  magnetic moments on this neutral fullerene. Doping with other lanthanide or actinide elements with suitable charge state can be used to stabilize a symmetric fullerene such as for  $M=Pa$  cation and  $M=Np$  anion. Among the neutral clusters we have studied, the BE is high (4.104 eV/atom) for  $M=Pa$  and the embedding energy of  $M$  atom in  $Si_{20}$  cage varies from about 8 eV to 14 eV, which is similar to the values obtained before<sup>2</sup> for other  $M$ -encapsulated silicon clusters.

Figure 3(a) shows the total pseudocharge density for  $M=Gd$  anion fullerene and the directional bonding between Si atoms can be seen. The distribution of the spin-polarization [Figs. 3(b) and 3(c)] shows that the moments are strongly localized around the Gd ion (total nearly  $7\mu_B$ ) and weak polarization of the same spin is induced around the eight neighboring Si ions forming a cube while the capping twelve

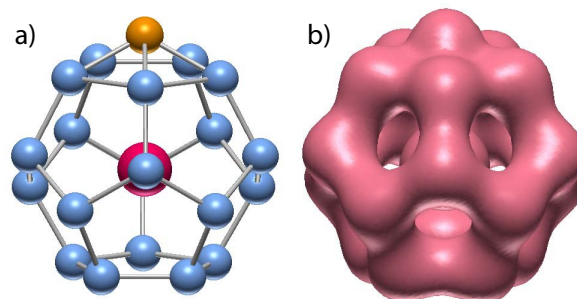


FIG. 4. (Color online) (a) Optimized structure of  $Cu-La@Si_{20}$  and (b) the isosurface of the total pseudocharge density. Cu is shown by brownish color. The density around Cu is mainly due to  $3d$  electrons.

ions develop weak polarization of the opposite sign. Similar localization of the magnetic moments has been found in other cases. This is indicative that local magnetic moment of the  $M$  atom can be preserved in the case such fullerenes can be assembled.

In order to further check the superhalogen behavior of some of these fullerenes, we calculated interaction of a Cu atom with the neutral  $\text{La@Si}_{20}$ . A Cu atom is placed on a face and the optimized structure has fivefold rotational symmetry. The gain in the BE is 2.90 eV, which is similar to the value for the electron affinity. Cu atom transfers charge to the cage. As shown in Fig. 4, the density around the Cu ion is mainly due to the  $3d$  electrons. The HOMO-LUMO gap is large with the value of 0.91 eV. The addition of Cu atom outside the cage leads to an increase in the neighboring Si-Si bond lengths to 2.50 Å in the corresponding pentagon. The Cu-Si bond length is 2.37 Å. A similar behavior is obtained for alkalis such as Na and Li and can be expected for Ag and Au. These results point to the possibility of forming salts of this silicon fullerene. Alkali doped clathrate structures are well known<sup>26</sup> in which alkali atoms occupy the vacant space in the silicon cages. Our results suggest the possibility of forming new phases of silicon by an appropriate mixing of a lanthanide and alkali/noble  $M$  atoms with silicon in the composition of  $\text{LMSi}_{20}$  where  $L$  is a trivalent atom as considered here and  $M$ , a monovalent  $M$  atom. Other suitable combinations could also become possible. Note that there are several examples<sup>27</sup> of Zintl phases of group 14 elements with isolated clusters by doping of alkali metals.

The strongly localized nature of  $f$  electrons could lead to significant orbital magnetic moments in these fullerenes. Considering the spin-orbit coupling and magnetization direction to be  $z$ , we find the orbital magnetic moment  $\langle L_z \rangle$  to be

$-0.37\mu_B$ ,  $-1.41\mu_B$ ,  $-0.2\mu_B$ , and  $2.41\mu_B$  for Pa, Sm, Gd (anion), and Tm, respectively. In general the orbital magnetic moment is significantly quenched and for Gd it is close to zero as also in atom. The magnetic anisotropy energy is very small ( $\sim$ meV) and the spin-magnetic moment is insensitive to the magnetization direction.

In summary we have reported stabilization of  $\text{Si}_{20}$  fullerene by encapsulation of a variety of metal atoms. Y, La, and Ac stabilize  $M@Si_{20}^-$  fullerene anion in the icosahedral symmetry. In other cases the  $\text{Si}_{20}$  cage has a dodecahedral structure with  $T_h$  symmetry or it is slightly Jahn-Teller distorted. This is the largest cage of silicon that can be stabilized by a metal atom. The high symmetry should lead to the additional stability as well. An important finding is that doping of lanthanides and actinides can be used to develop magnetic fullerenes of silicon. Gd doped fullerene anion is predicted to have a high magnetic moment of  $7\mu_B$ . The large HOMO-LUMO gap ( $\sim$ 1 eV) can be expected to give rise to the high abundances of the fullerenes. Trivalent La, Y, or Ac as well as Gd doped fullerenes are superhalogens and interaction with alkali or noble metal atoms could lead to new phases of silicon based fullerides as it has been the case for  $\text{C}_{60}$ . Such silicon fullerenes also have potential to develop new silicon based molecular structures and nanoscale magnetic species. We hope that our findings will stimulate experimental work to produce these fullerenes in laboratory and their derivatives as well as functional nanostructures.

V.K. is thankful for the kind hospitality at the Institute for Materials Research; RICS, AIST; and the Institute of Mathematical Sciences, Chennai. A.K.S. gratefully acknowledges the support of Japan Society for Promotion of Science (JSPS).

\*Present address: Materials Department, University of California Santa Barbara, Santa Barbara CA 93106.

<sup>1</sup>S. M. Beck, J. Chem. Phys. **87**, 4233 (1987); **90**, 6306 (1989).

<sup>2</sup>V. Kumar and Y. Kawazoe, Phys. Rev. Lett. **87**, 045503 (2001); **91**, 199901(E) (2003).

<sup>3</sup>H. Hiura, T. Miyazaki, and T. Kanayama, Phys. Rev. Lett. **86**, 1733 (2001).

<sup>4</sup>V. Kumar and Y. Kawazoe, Phys. Rev. B **65**, 073404 (2002); T. Miyazaki, H. Hiura, and T. Kanayama, *ibid.* **66**, 121403 (2002); J. Lu and S. Nagase, Phys. Rev. Lett. **90**, 115506 (2003); S. N. Khanna, B. K. Rao, and P. Jena, *ibid.* **89**, 016803 (2002); G. Mpourmpakis, G. E. Froudakis, A. N. Andriotis, and M. Menon, Phys. Rev. B **68**, 125407 (2003); W. Zheng, J. M. Nilles, D. Radisic, and K. H. Bowen, J. Chem. Phys. **122**, 071101 (2005); H. Kawamura, V. Kumar, and Y. Kawazoe, Phys. Rev. B **71**, 075423 (2005).

<sup>5</sup>V. Kumar, Comput. Mater. Sci. **30**, 260 (2004) and references therein.

<sup>6</sup>V. Kumar, A. K. Singh, and Y. Kawazoe, Nano Lett. **4**, 677 (2004); V. Kumar and Y. Kawazoe, Phys. Rev. Lett. **88**, 235504 (2002).

<sup>7</sup>V. Kumar and Y. Kawazoe, Appl. Phys. Lett. **83**, 2677 (2003).

<sup>8</sup>K. Koyasu, M. Akutsu, M. Mitsui, and A. Nakajima, J. Am.

Chem. Soc. **127**, 4998 (2005); M. Ohara, K. Koyasu, A. Nakajima, and K. Kaya, Chem. Phys. Lett. **371**, 490 (2003).

<sup>9</sup>S. Neukermans, E. Janssens, Z. F. Chen, R. E. Silverans, P. v. R. Schleyer, and P. Lievens, Phys. Rev. Lett. **92**, 163401 (2004).

<sup>10</sup>E. N. Esenturk, J. Fettinger, and B. Eichhorn, Chem. Commun. (Cambridge) 247 (2005).

<sup>11</sup>M. Harada, S. Osawa, E. Osawa, and E. D. Jemmis, Chem. Lett. **1**, 1037 (1994).

<sup>12</sup>E. D. Jemmis, J. Leszczynski, and E. Osawa, Fullerene Sci. Technol. **6**, 271 (1998).

<sup>13</sup>E. F. Sheka, E. A. Nikitina, V. A. Zayets, and I. Y. Ginzburg, Int. J. Quantum Chem. **88**, 441 (2002).

<sup>14</sup>H. Tanaka, S. Osawa, J. Onoe, and K. Takeuchi, J. Phys. Chem. B **103**, 5939 (1999).

<sup>15</sup>X. G. Gong and Q. Q. Zheng, Phys. Rev. B **52**, 4756 (1995).

<sup>16</sup>Q. Sun, Q. Wang, P. Jena, B. K. Rao, and Y. Kawazoe, Phys. Rev. Lett. **90**, 135503 (2003).

<sup>17</sup>K. Jackson and B. Nellermore, Chem. Phys. Lett. **254**, 249 (1996).

<sup>18</sup>Q. Sun, Q. Wang, T. M. Briere, V. Kumar, Y. Kawazoe, and P. Jena, Phys. Rev. B **65**, 235417 (2002); T. Nagano, K. Tsumuraya, H. Eguchi, and D. J. Singh, *ibid.* **64**, 155403 (2001).

- <sup>19</sup>A. K. Singh, V. Kumar, and Y. Kawazoe, *Phys. Rev. B* **71**, 115429 (2005).
- <sup>20</sup>F. A. Cotton, G. Wilkinson, C. A. Murillo, and M. Bochmann, *Advanced Inorganic Chemistry*, 6th ed. (John Wiley and Sons, Inc., New York, 1999).
- <sup>21</sup>G. Kresse and J. Joubert, *Phys. Rev. B* **59**, 1758 (1999).
- <sup>22</sup>P. Blöchl, *Phys. Rev. B* **50**, 17953 (1994).
- <sup>23</sup>J. P. Perdew, in *Electronic Structure of Solids '91*, edited by P. Ziesche and H. Eschrig (Akademie Verlag, Berlin, 1991).
- <sup>24</sup>W. B. Pearson, *The Crystal Chemistry and the Physics of the Metal Alloys* (Wiley, New York, 1982).
- <sup>25</sup>K. Jackson, E. Kaxiras, and M. R. Pederson, *J. Phys. Chem.* **98**, 7805 (1994).
- <sup>26</sup>F. Tournus, B. Masenelli, P. Mélinon, D. Connétable, X. Blasé, A. M. Flank, P. Lagarde, C. Cros, and M. Pouchard, *Phys. Rev. B* **69**, 035208 (2004) and references therein.
- <sup>27</sup>S. Bobev and S. C. Sevov, *Angew. Chem., Int. Ed.* **39**, 4108 (2000).